Design of a liquid scintillator-based prototype neutron coincidence counter for Nuclear Safeguards

Alice Tomanin[1,2], Paolo Peerani[1], Hamid Tagziria[1], Greet Janssens-Maenhout[2], Peter Schillebeeckx[3], Jan Paepen[3], Anthony Lavietes[4], Romano Plenteda[4], Nicholas Mascarenhas[4], L. Marie Cronholm[4]

1. European Commission - Joint Research Centre - Institute for Transuranium Elements - Nuclear Security Unit, Ispra, Italy
2. University of Ghent, Ghent, Belgium
3. European Commission - Joint Research Centre - Institute for Reference Materials and Measurements - Standards for Nuclear Safety, Security and Safeguards Unit, Geel, Belgium.
4. International Atomic Energy Agency, Vienna, Austria

E-mail: alice.tomanin@jrc.ec.europa.eu

Abstract:

A liquid scintillator-based neutron coincidence counting system designed to address a number of safeguards applications is under development by the IAEA in collaboration with the Joint Research Centre-ITU and Hybrid Instruments LTD.

Liquid scintillators are a promising technology due to their good fast-neutron detection capabilities. The characteristic fast response of scintillators is particularly beneficial for coincidence counting applications, for which a performance level higher than that associated with moderated thermal detectors might be expected. Fast neutron detection requires no thermalization process and therefore, does not incur the resulting neutron detection delays. These features reduce the length of the coincidence gate by three orders of magnitude, reducing practically to negligible values the accidental coincidence rate which dominates the uncertainty in thermal neutron detectors. Recent progress in fast electronic digitizers offers the possibility to perform on-line, real-time pulse shape discrimination (PSD) between gamma and neutron radiation detection, making this technology suitable for nuclear safeguards and security applications.

This paper will describe the experiments and Monte Carlo modelling activities engaged to design a prototype liquid scintillator-based neutron coincidence collar for fresh fuel assembly verification.

The characterization of the system response required accurate calibration measurements in order to determine the operational parameters of the liquid scintillator cell, including gain, pulse shape discrimination and energy thresholds.

Extensive Monte Carlo simulations which are essential for the understanding and characterization of the system's response were also carried out using the MCNPX-PoliMi Monte Carlo code to simulate the radiation transport within the system and to optimize the detector design. The evolution from the different detector configurations we investigated to the characteristic features of the final design will be described.

Keywords: non-destructive assay; neutron detection; coincidence counting; liquid scintillators; Monte Carlo modelling.

1. Introduction

Neutron coincidence counting is a well-known measurement technique commonly used in nuclear safeguards for the verification of the declared quantity of special nuclear material.

The technique relies on the detection of time-correlated neutrons from either spontaneous or neutron induced fissions occurring in a nuclear material containing fissile or fissionable material such as uranium and plutonium. In the presence of a well-known calibration curve, the rate of coincident neutron detection events can be directly related to the mass of such isotopes in the investigated material.

In order to detect neutrons, currently deployed coincidence counters rely on the use of ^{3}He gas, due to its high cross section for thermal neutron captures and low sensitivity for gamma-rays. The recently increased demand for ^{3}He-based neutron detectors, in particular for nuclear security applications, coupled with the limited production of ^{3}He, has made this gas practically unavailable, creating the need to search for alternative neutron detection solutions.

The International Atomic Energy Agency, in collaboration with the Joint Research Centre - Institute for Transuranium Elements and Hybrid Instruments LTD is developing a liquid scintillator-based neutron coincidence counter to replace the current deployed systems for safeguards applications.

The choice of liquid scintillators as a suitable ^{3}He alternative for this particular application was motivated by the very fast response of this detection medium. In addition, improved performance as compared to classical ^{3}He counters is expected with regard to measurement time and related statistics. Fast neutron detection requires no thermalization process and therefore, does not incur the resulting neutron detection delays (i.e., die-away time). These features reduce the length of the coincidence gate by three orders of magnitude, reducing practically to negligible values the accidental coincidence rate which dominates the uncertainty in thermal neutron detectors. Recent

progress in fast electronic digitizers offers the possibility to perform on-line, real-time pulse shape discrimination (PSD) between gamma and neutron radiation detection events, making this technology suitable for nuclear safeguards and security applications.

The characterization of the performance of the system and its design optimization were performed by means of Monte Carlo simulations. Simulations were performed with the MCNPX-PoliMi code [1], a Monte Carlo modelling tool developed to simulate detectors response, combined with a post-processing code developed at the JRC-ITU Ispra. Prior work in post processing for liquid scintillator was taken as reference in the development of the JRC code [2]. Due to the expected non-linearity of the light output function (LOF) of a scintillator, i.e. non-linear transfer of the deposited energy to the light output, each single collision occurring within the effective detection volume has to be evaluated separately. Depending on the incident particle type and the target atom, the energy deposited is converted into scintillation light with the detector-specific light conversion formula. The amount of light produced by subsequent collisions occurring within a specific pulse-rise time are summed to generate pulses which are then processed by the PSD electronics. The post-processor code includes modules to apply the conversion from deposited energy to light and to identify coincident events within multiple detector cells. A validation of the simulations was performed on a small scale coincidence system (composed of two liquid scintillator cells) proving that the modelling reproduces the expected detector response.

2. Liquid scintillator cell characterization

2.1 Measurements set-up

The prototype system is composed of an array of EJ-309 liquid scintillator cells, with cubic geometry of 10 cm width, a multichannel real-time pulse shape discrimination (PSD) system, and a high-speed data acquisition and signal processing system to compute coincidences. The detailed design and electronics setup is discussed by Lavietes et al. [3].

A prototype liquid scintillator cell which has the same geometry and size as the one we foresee to use for the full-scale system was characterized at the JRC-ITU laboratories in Ispra, at the JRC-IRMM in Geel as well as at the PTB facilities in Braunschweig, Germany. Radionuclide gamma sources and monoenergetic neutron beams were used in order to determine the response of the detector to different radiation types and energies. In the following section only the results obtained at JRC-ITU are discussed.

For the coincidence validation measurements, a second EJ-309 liquid scintillator of cylindrical geometry (5 inches diameter and 3 inches length) was used.

2.2 Operating Voltage

The selection of the optimal operating voltage for the detector was primarily based on a study of the detector resolution and linearity of the response to gamma rays. Measurements were performed with a ^{137}Cs, ^{22}Na and ^{232}U source. Figure 2 shows the measured relative FWHM at the Compton edge with respect to the applied voltage for three gamma energies. In addition, an AmBe (α,n) source was used to determine the response for higher energy gamma rays (Compton edge energy 4201 KeV) and to verify the performance of the detector with respect to pulse shape discrimination. As expected, the resolution improves by increasing the high voltage. The best resolution and linearity of the detector response was observed at -1250 V. Measurements with the AmBe neutron source confirmed that this voltage also results in an optimal performance with respect to pulse shape discrimination.

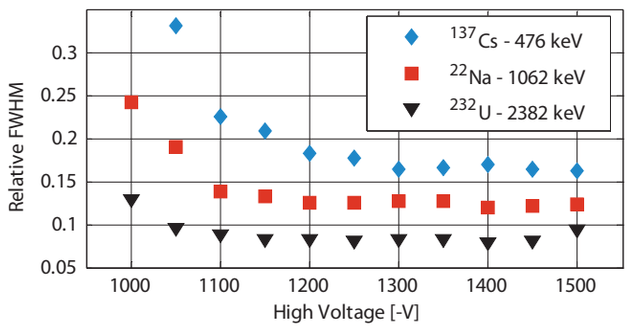

Figure 1. Relative FWHM with respect to applied High Voltage for three different Compton edge energies.

2.3 Pulse Shape Discrimination

The pulse shape discrimination (PSD) electronics implemented in the system is based on a comparison of the peak amplitude to the amplitude in the decay face of the pulse, i.e. the amplitude at 16 ns after the peak. The latter is referred to as discrimination amplitude. This approach allows for real-time discrimination between gamma and neutron detection events.

The performance of the PSD technique for measurements with a ^{252}Cf source is illustrated in Fig. 2. For each detected event the peak amplitude is plotted as a function of the discrimination amplitude. In this plot two clouds of events can be observed. The discrimination between the two clouds is given by a line with two segments, defined by the points A, B and C. Based on this discrimination criterion events due to the detection of a neutron (blue points) can be separated from those resulting from the detection of a gamma ray (red points).

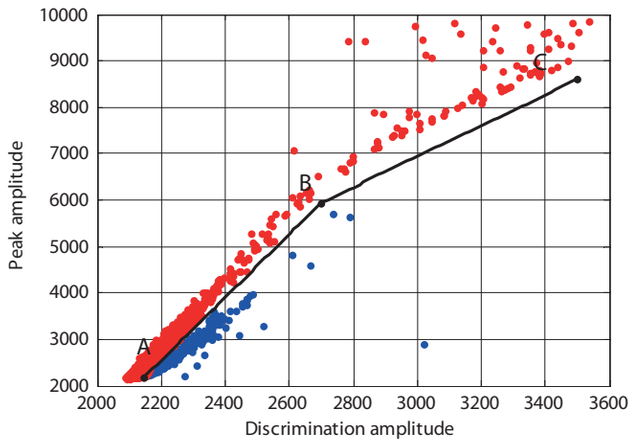

Figure 2. Typical PSD graph for a ^{252}Cf measurements. Gamma pulses are shown in red, neutron pulses in blue. Amplitudes as measured in digitizer units.

Optimization of the PSD was obtained by varying the slope of the A-B discrimination line (i.e. by variation of the x-coordinate of the A point), and analyzing the PSD response of the system in terms of neutron intrinsic efficiency and gamma rejection rate. The gamma rejection rate (GARR), defined as the ratio of misclassified neutrons in the presence of a pure gamma source to the totals detected pulses, can be written as:

$$GARR = \frac{Neutrons}{Neutrons + Gammas}$$

It is well known that the most probable misclassification of neutron and gamma events occurs in the low energy region, therefore the GARR was computed for a measurement with an ^{241}Am source. Background neutrons are included in the total neutron counts for the calculation of the GARR. However, in the low energy region, their contribution is negligible since the most neutron counts are given by misclassified gammas. The intrinsic efficiency values are derived by a measurement with a ^{252}Cf source. For these measurements, the light energy threshold, which will be described in more detail in a following section, was set to 385 electron equivalent keV (keVee, i.e. light generated by an electron depositing 1 keV of energy in the scintillator). Figure 3 represents the resulting Figure of Merit of this analysis. The resulting PSD settings were determined by an optimization of neutron detection efficiency and gamma rejection. For the selected setting, the neutron intrinsic efficiency is 14% and the GARR is 0.05%.

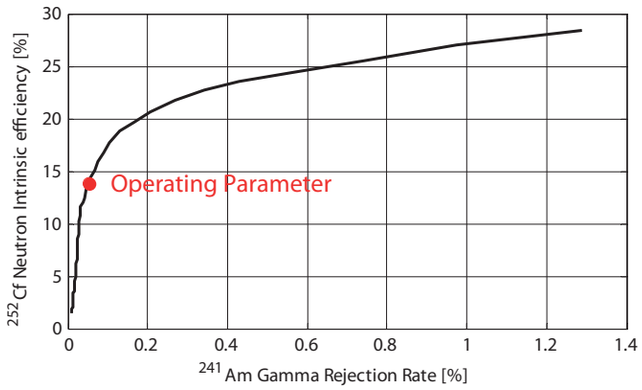

Figure 3. PSD Figure of Merit showing the GARR and the neutron intrinsic efficiency response at the variation of the Ax discrimination parameter. The red circle represents the operating parameter.

2.4 Validation of simulated detector response

The scintillation response of the detector, in terms of light production per incident particle and energy, is required for reliable simulation of the detector's response. Liquid scintillators typically present a linear response for gammas, whereas the light produced by protons and heavier particles varies non-linearly with the energy deposited [4]. The light output function (LOF) for recoil protons (the detection mechanism for neutrons) depends on the liquid type, the cell geometry and the cell–photomultiplier coupling. The LOF for cylindrical EJ-309 liquid scintillator of different diameters has been already reported by Pozzi et al. [5, 6], but the particular geometry of our detector requires a specific derivation of its light response.

The calibration measurements were performed at the PTB laboratories in Braunschweig, Germany, and consisted in time-of-flight measurements using the PTB cyclotron and measurements with quasi-monoenergetic neutron beams at the PTB Van Der Graaff accelerator. Further

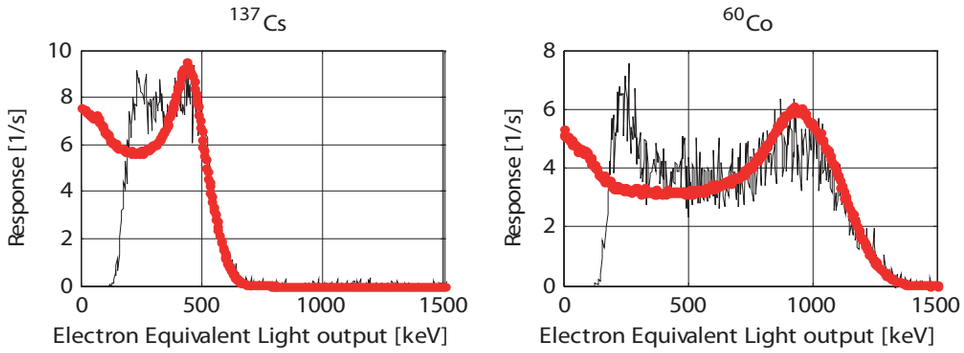

Figure 4. Measured (black line) and simulated (red dots) pulse height spectra for a ^{137}Cs source (left) and a 60Co source (right).

measurements were performed at the JRC-IRMM in Geel and at the JRC-ITU in Ispra to verify the experimental LOF against full neutron spectra from AmBe and AmLi sources. The analysis of the data is still in progress. We report here on results obtained with a LOF obtained following a preliminary analysis of the data. A detailed discussion on the results of these experiments together with the experimental response matrix and resulting LOF for electrons and protons will be subject of a separate publication.

The results of the Monte Carlo simulations have been validated by comparing the simulated and experimental response for gamma rays from a ^{137}Cs and ^{60}Co source and for neutrons from a ^{252}Cf spontaneous fission source. The results of the gamma ray measurements were used to determine the conversion factor that relates the observed amplitude to an electron equivalent light output for the data acquisition system.

Figure 4 compares the measured and simulated pulse height spectra for ^{137}Cs and ^{60}Co sources. The positions of the Compton edges observable in the graphs are shifted with respect to the true Compton edges values by the detector resolution. Above a light output of approximately 380 electron equivalent keV there is a good agreement between the shape of the simulated and experimental response. The simulated response, however, is overestimated by at least 15%. This bias is much larger than the uncertainty due to the counting statistics on the detection efficiency, which is about 2%. This bias is probably due to an overestimation of the effective detection volume, i.e. the effective volume of the scintillation liquid. Below a light output of about 380 keV the simulated response is lower compared to the experimental one. This might be due to a background component that is not properly accounted for or due to noise on the detector signal introduced by the electronics.

Fig.5 compares the simulated and experimental response for the detection of neutrons emitted by a ^{252}Cf source as a function of the light output. The figure indicates a good agreement in shape above 600 keV electron equivalent light output.

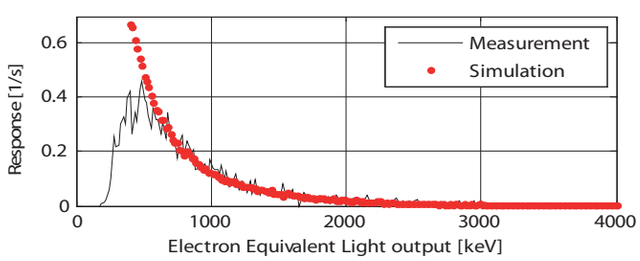

Figure 5. Measured (black line) and simulated (red dots) neutrons pulse height spectra for a Cf_{252} source.

2.5 Energy threshold

A fundamental parameter to use the scintillation detector as part of a counting system for the control of nuclear material is the energy threshold or discrimination level on the light output. This level, which reflects the minimum detectable light output, is an adjustable parameter of the electronic settings.

The pulse height spectrum shown in figures 4 and 5 were taken with the minimum electronic threshold setting. This level was choosen to reduce the noise to an acceptable level compared to the measured signal. The threshold used in the counting experiments corresponds to the minimum light output where the calculated spectrum still agrees with the experimental values.

As can be noted in Figures 4 and 5, the threshold of the electronics used does not result in a sharp edge on the left side of the pulse height spectrum, but it rather presents some broadening effect. This effect is due to a systematic behavior of the acquisition electronics, which introduces a bias in the threshold determination. Further developments in the acquisition electronics are planned in order to address this issue.

In this work, we derived the energy threshold value with a different approach, that is by matching the integral of the simulated response evaluated at different low energy thresholds with the total measured counts. Considering the pulse height spectra for ^{252}Cf reported in figure 5, the value that matches the counts, and thus validates the simulations for the neutron intrinsic efficiency of the detector, was found to be 385 electron equivalent keV, corresponding to a neutron energy of approximately 1.6 MeV. For the investigated detector and for the described setup we observed quite poor performance with respect to neutron detection efficiency at low energies, meaning that the minimum detectable energy is, by default, very high. Further adjustments in the electronic settings can only be applied to increase this threshold. However, this limit is strongly related to the electronics that is used and does not correspond to the lower limit due to the intrinsic detector characteristics. A possible solution to decrease the lower limit is to either use electronics with different dynamic ranges or increase the high voltage and use multiple outputs at different stages of the photo-multiplier tube.

2.6 Validation of coincidence on a two-cell detection system

In order to validate the procedure to simulate coincident events, measurements were carried out with two liquid scintillator cells, a ^{252}Cf source placed at 10 cm from each cell, and increasing thicknesses of lead shielding to study the effect of gamma pile-up. The second cell used for these measurement was a cylindrical 5'' x 3'' EJ-309 scintillator. For the simulation of the cylindrical detector response, the light output function was taken from literature data [5] whereas its energy threshold was set to 155 electron equivalent keV. Fig. 6 shows a part of the experimental set-up.

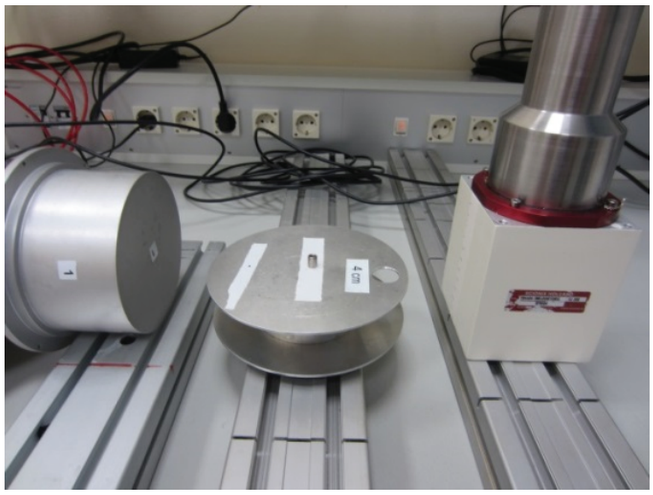

Figure 6. Experimental configuration for the coincidence validation measurements with Cf_{252}. The source to detector distance is 10 cm.

Results of the validation measurements and simulations are shown in figure 7. While the total count rate is overestimated by about 5-10% in the results (and is explained by the effective scintillator volume overestimation discussed in par. 2.4), the real count rates are underestimated by a factor of about 20%. This inconsistency in system response will be further analyzed in a wider range of neutron energies with coincidence validation experiments using plutonium oxides and AmLi sources to evaluate cross-talk effects.

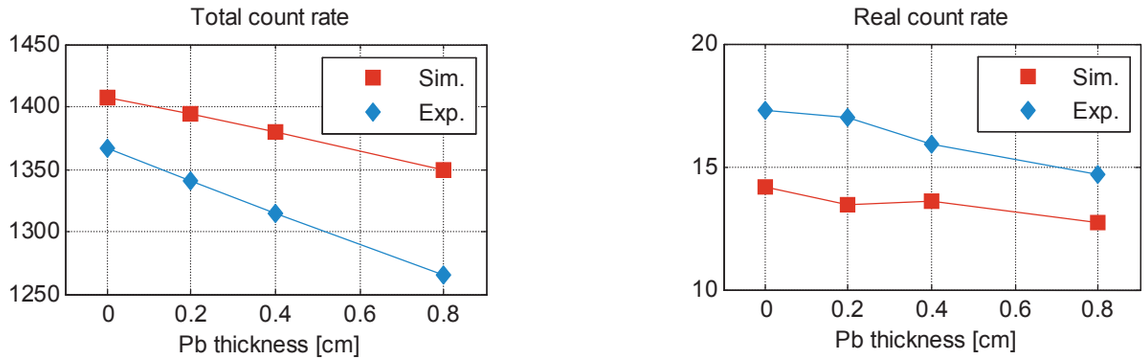

Figure 7. Measured and simulated totals (left) and reals (right) counts rates for the coincidences validation measurements with 252Cf and different lead shielding of different thicknesses. Real count rates are corrected for Accidentals coincidences.

3. Response of the full-system prototype

Figure 8 (left) shows the proposed design of the prototype liquid scintillator based coincidence collar.

It comprises 12 liquid scintillator cells of approximately 1 liter volume each, arranged on three sides of the collar. The fourth side is designed to accommodate an AmLi interrogation source. The cells and source are embedded in a 10 cm thick high density polyethylene (HDPE) wall to moderate the neutrons from the AmLi source. Moderation of the interrogating neutrons will result in decrease of the average energy and consequently in a substantial increase of the average cross section for neutron induced fission in the fuel assembly. A 1 cm HDPE interspace between neighboring cells is foreseen to reduce cross-talk events. The internal cavity accommodating the fuel element is surrounded by a 4 mm layer of lead to reduce the gamma rate at the detectors and by a removable 1 mm thick layer of cadmium used to switch the system to a “fast” configuration when measuring fuel assemblies with neutron poison. The fast configuration significantly reduces the neutron poison effects by absorbing interrogation neutrons below the cadmium cut-off energy of about 0.55 eV.

Extensive MCNPX-PoliMi simulations were performed to characterize the system response and optimize the design. For this study, a typical PWR fuel element has been modeled. The data of the modeled fuel as well as the intensity of the interrogation source were taken from [7]. Figure 8 (right) shows a section of the simulated geometry perpendicular to the fuel element length.

In the next sections the total count rate is denoted by T, the net coincident count rate by R and the count rate due to accidental coincident events by A.

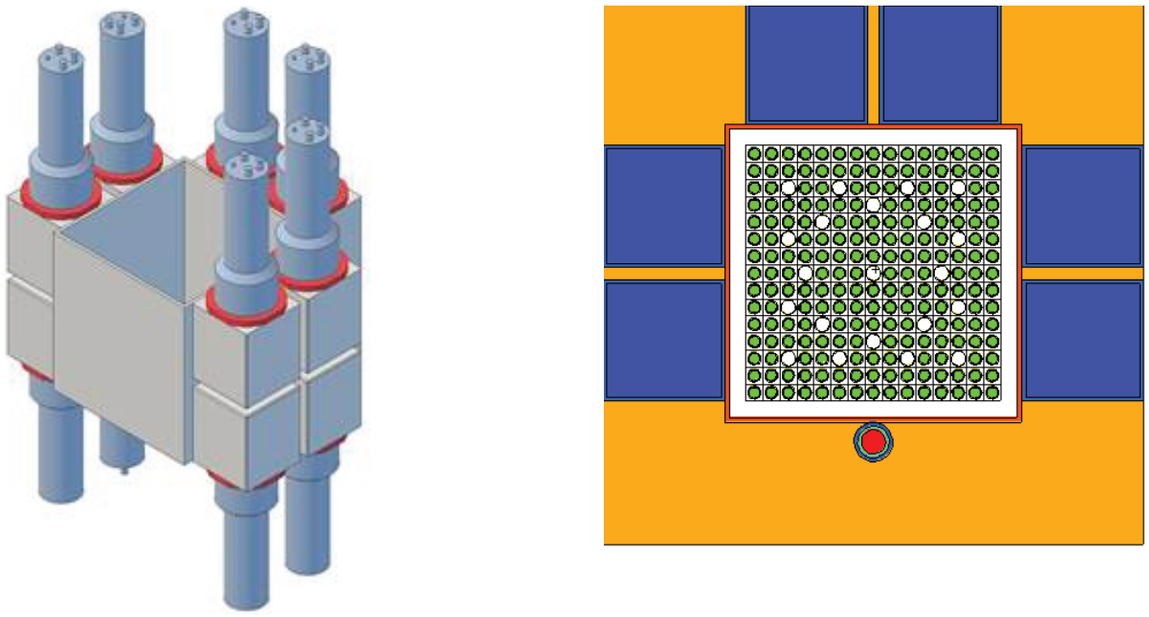

Figure 8. Prototype design of the liquid scintillator based coincidence collar (left, bare configuration without surrounding HDPE) and simulated geometry with MCNPX-PoliMi (right, thermal configuration with surrounding HDPE), containing reference fuel element and AmLi interrogation source.

In thermal neutron coincidence counters, for a given measurement time t, the uncertainty due to counting statistics on the Reals count is dominated by the Accidental count which is, in its turn, driven by the interrogation source:

$$\frac{\sigma}{R} = \frac{\sqrt{2A + R}}{R \cdot \sqrt{t}}$$

This effect leads to poor statistics and thus long measurement times which are necessary in order to achieve the 1% uncertainty due to counting statistics. One intrinsic advantage of liquid scintillators is that the exceptionally short coincidence window given by the detection of fast neutrons leads to smaller accidental rates. To give an example, the coincidence time gates in liquid scintillator is of the order of tens of nanoseconds, whereas tens of microseconds are needed in ^{3}He systems as to account for the neutron thermalization process.

3.1 Background from interrogating neutron source

A first analysis was performed to determine the interrogation source background (no fuel element in the detector) for three different configurations: a bare configuration (no surrounding HDPE); a thermal configuration (10 cm thick HDPE walls on each side of the collar); and a fast configuration (1 mm internal layer of cadmium to prevent interrogation with neutrons with an energy below 0.55 eV). The analyses were performed at different energy thresholds to define the optimal operating condition of the collar. Figure 9 shows the results of the simulation.

The contribution from the AmLi neutron source to coincident count rate results mainly from neutrons which are scattered from one detector to another. In such cases one neutron produces a signal in different detectors. This is also referred to as cross-talk between detectors.

The bare configuration presents steadily higher influences of the interrogation neutrons on the Real count rates. This is given by the absence of HDPE-filled interspace between neighboring detectors, which act both as a support material for the cells, and as a moderator for the neutrons which do not come directly from the fuel element cavity, reducing their probability of being detected by the scintillators.

As a result of this analysis, the bare configuration has been discarded, and two possible operating settings were identified for the following analysis on the thermal and fast configuration:

- 0.5 MeV neutron energy threshold: this operational setting reduces to negligible values the cross-talk effect of the interrogating source neutrons on the count rate of the Reals. This would allow the detector to be calibrated against the count rate of the Reals, as in current 3He system, minimizing the AmLi source driven Accidentals.
- 1 MeV to 1.5 MeV neutron energy threshold: this operational setting reduces to negligible values the influence of the interrogating source neutrons on the count rate of the Totals. We intend to investigate the possibility of calibrating the detector against the count rate of the Totals, which are no longer driven by the AmLi interrogation source, in order to achieve better statistics in shorter measurement time. When using the Totals data, the count rate of the Reals would be used as a control information to confirm the uranium enrichment of the fuel element and verify the absence of any nearby uncorrelated neutron source intended to bias the measurements results in an unattended operational mode.

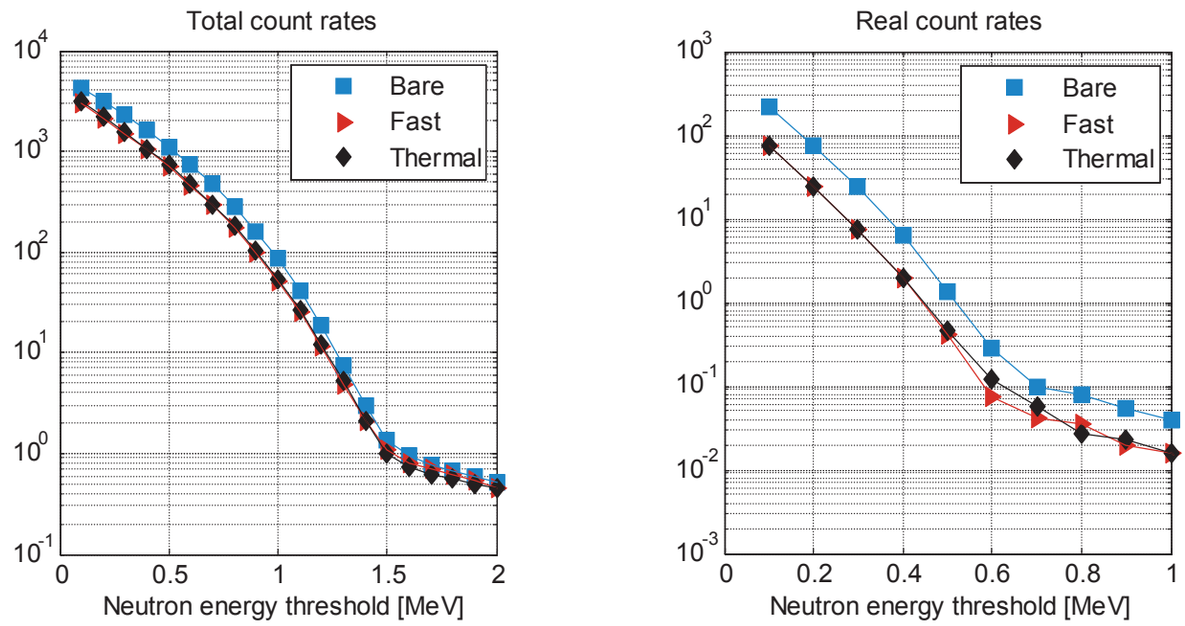

Figure 9. Simulated totals (left) and reals (right) counts rates for the liquid scintillator-based collar in three different configurations: bare, thermal, and fast. The counts are given only by the AmLi interrogation source – no fuel assembly is present. Thresholds are expressed in neutron energy for simplification.

3.2 Prototype response for the verification of a PWR fuel assembly

Table 1 shows results of the simulation performed on the neutron coincidence collar for the fuel assembly interrogation, and for two defined configurations and at three different threshold settings. The enrichment of the fuel is 3.19 wt%. The uncertainties resulting from only counting statistics of all the presented data are below 1%.

Concerning the reals count rates, we observed for both configurations that a neutron energy threshold of 0.5 MeV is sufficient to reduce the influence of AmLi neutrons cross-talk to about 1%.

The resulting count rates are then directly related to the induced fissions in the fuel assembly, and a counting statistics uncertainty of 1% can be achieved in a few minutes.

In absolute values, the AmLi source neutrons detected by the scintillators in both configurations are the same, as it results from figure 9. In the fast configuration, however, the cadmium layer within the cavity reduces the probability of AmLi neutrons to induce fissions in the fuel assembly, and thus the neutron count rates related to induced fissions in the fuel. Consequently, the relative influence of the interrogation source neutrons is higher in the fast configuration, requiring a higher energy threshold of up to 1.5 MeV (neutron energy) to reduce the AmLi contribution to approximately 1% of the Totals count rate. At this threshold, less than 4 minutes measurement would be necessary to obtain the counts of the Totals at less than 1% relative counting statistics uncertainty. In the same measurement time, the counts of the Reals would be determined with a 5% uncertainty, providing a good indication regarding the absence of any uncorrelated sources nearby the collar which would bias the measurement.

Table 1. Simulation of the system response in the proposed configurations and three different threshold settings for a 3.19 wt% enriched fuel element interrogation. Counting statistics uncertainties of the results are below 1%. Thresholds are expressed in neutron energy for simplification.

Threshold	Thermal configuration				Fast configuration			
	T [1/s]	T_{AmLi}	R [1/s]	R_{AmLi}	T [1/s]	T_{AmLi}	R [1/s]	R_{AmLi}
0.5 MeV	1443	20 %	150	0.12 %	634	70 %	23.0	1.07 %
1.0 MeV	578	3 %	39	0.02 %	119	23 %	6.0	0.23 %
1.5 MeV	313	0.13 %	12	0.02 %	51	1.25 %	1.7	0.16 %

3.3 Comparison with ^{3}He-based systems

In the following section we present a comparison of the coincidence collar capabilities with those of a classical ^{3}He thermal coincidence collar.

We simulated the response of two commercially available ^{3}He based system, the JCC73 and the JCC71 models [8], to the same fuel and the same interrogation source intensity simulated in the liquid scintillator analysis. Data were simulated with the MCNP-pta code [9], that postprocesses the coincidence counters response. The results are presented in table 2.

Table 2. Simulation of the response of two typical ^{3}He based neutron coincidence collars in thermal and fast configuration for a 3.19 wt% enriched fuel element interrogation.

Configuration	JCC73			JCC71		
	T[1/s]	R [1/s]	A [1/s]	T[1/s]	R [1/s]	A [1/s]
Thermal	2900	190	538	2100	124	282
Fast	1200	12	92	800	6	41

Table 3 and 4 provide a direct comparison of the achieved counting statistic uncertainty of the two systems for both thermal and fast configuration interrogation at different measurements times. Fast configuration is usually more time-consuming than the thermal configuration, therefore it is the most critical for this analysis.

Table 3. Counting statistics uncertainty related to different measurement times for the ^{3}He based JCC73 and for the liquid scintillator-based coincidence counter, both in thermal configuration. Results for the liquid scintillator- based prototype are reported for the Reals mode (threshold set to 0.5 MeV neutron energy) and for the Totals mode (threshold set to 1.5 MeV neutron energy).

Measurement time	JCC73 σ [%]	LS Reals σ [%]	LS Totals σ [%]
60 s	2.3	1.0	0.7
600 s	0.7	0.3	0.2

Table 4. Counting statistics uncertainty related to different measurement times for the ^{3}He based JCC73 and for the liquid scintillator-based coincidence counter, both in fast configuration. Results for the liquid scintillator- based prototype are reported for the Reals mode (threshold set to 0.5 MeV neutron energy) and for the Totals mode (threshold set to 1.5 MeV neutron energy).

Measurement time	JCC73 σ [%]	LS Reals σ [%]	LS Totals σ [%]
60 s	14.6	2.7	1.8
600 s	4.6	0.9	0.6
1 h	1.9	0.4	0.2
10 h	0.6	0.1	< 0.1

The advantage of fast neutron detection in liquid scintillators is clearly reflected in the results: it shows a consistent saving in measurement and operational time for the prototype system.

4. Conclusions

This paper provides data for the use of liquid scintillators as effective 3He replacement technology for nuclear safeguards applications, given their good neutron detection efficiency and gamma ray rejection capabilities.

We proposed an optimized design for a prototype liquid scintillator-based neutron coincidence collar made of 12 liquid scintillator cells.

Systematic effects, such as stability of the response with respect to high voltage small drifts and environmental changes, have not been evaluated in this paper and are planned for future work.

The capabilities of the system were analyzed by Monte Carlo simulations using MCNPX-PoliMi code, which proved to be an essential tool for simulating the detector response.

The system modelling required accurate characterization of the liquid scintillators cell response in terms of light output production for different incident particles and energies, and these functions needed to be evaluated separately for each cell geometry.

Finally, a comparison of the proposed prototype with existing 3He based systems shows promising fast neutron detection characteristics of the liquid scintillator, which is advantageous in terms of measurement time and related statistics, two very important factors in nuclear safeguards applications.

5. Acknowledgements

The authors would like to thank Raft Nolte (PTB, Braunschweig) for its kind support in the characterization of the detector. The authors would also like to acknowledge professor Padovani (Polytechnic university of Milan, Italy),

professor Pozzi, Jennifer Dolan and Eric Miller(University of Michigan, MI, USA) for their support during the set-up of the simulations and the implementation of the JRC post-processor code.

6. References

[1] E.Padovani, S.A.Pozzi, S.D.Clarke, E.C.Miller, MCNPX-PoliMi User's Manual, C00791 NYCP, Radiation Safety Information Computational Center, Oak Ridge National Laboratory, 2012.

[2] S. Pozzi, E. Padovani, M. Flaska, and S. Clarke (2007). MCNP-PoliMi Post-Processing Code Ver. 1.9. Oak Ridge National Laboratory Internal Report, ORNL/TM-2007/33

[3] Liquid scintillator-based neutron detector development, A. Lavietes, R. Plenteda, N. Mascarenhas, L. M. Cronholm, M. Aspinall, M. J. Joyce, A. Tomanin, P. Peerani, submitted to IEEE Transaction on Nuclear Science, forthcoming 2013.

[4] The theory and practice of scintillation counting, J. B. Birks, Pergamon Press, 1964.

[5] Optimization of a Mixed Multiplicity Counter Using Monte Carlo Simulations and Measurements, A. Enqvist, K. Weinfurther, M. Flaska,S. Pozzi, IEEE Transaction on Nuclear Science, 2010.

[6] Neutron Light Output Response and Resolution Functions in EJ-309 Liquid Scintillation Detectors, A. Enqvist, C. C. Lawrence, B. M. Wieger, S. A. Pozzi, T. N. Massey, Nucl. Instr. Meth. A 715 (2013) p. 79

[7] MCNPX-based determination of UNCC correction factors (Benchmark problems for MCNPX simulation), S. Y. Lee, D. H. Beddingfield, LA-UR-09-03573

[8] Monte Carlo simulation of neutron counters for safeguards applications, M. Looman, P. Peerani, H. Tagziria, Nucl. Inst. Meth. A 598 (2009) p. 542-550.

[9] M.R. Looman, N. Farese, G. Gonano, R. Jaime, B. Pedersen, and P. Schillebeeckx, "Monte Carlo Prediction of the Response of Neutron Counting Instruments", Proceedings of the 21th Annual Symposium on Safeguards and Nuclear Material Management, Seville, Spain, 4 – 6 May 1999, ESARDA Proceedings 29 (1999) pp. 375-381